ELSEVIER

Journal of Nuclear Materials 273 (1999) 213–220

journal of nuclear materials

www.elsevier.nl/locate/jnucmat

Neutron irradiation induced amorphization of silicon carbide

L.L. Snead *, J.C. Hay [1]

Metals and Ceramics Division, Oak Ridge National Laboratory, Oak Ridge, TN 37830-6087, USA

Received 22 May 1998; accepted 29 December 1998

Abstract

This paper provides the properties of bulk stoichiometric silicon carbide which has been amorphized under neutron irradiation. Both high purity single crystal hcp and high purity, highly faulted (cubic) chemically vapor deposited (CVD) SiC were irradiated at approximately 60°C to a total fast neutron fluence of 2.6×10^{25} n/m^2. Amorphization was seen in both materials as evidenced by TEM, electron diffraction and X-ray diffraction techniques. Physical properties for the amorphized single crystal material are reported including large changes in density (−10.8%), elastic modulus as measured using a nanoindentation technique (−45%), hardness as measured by nanoindentation (−45%), and standard Vickers hardness (−24%). Similar property changes are observed for the amorphized CVD SiC. Using measured thermal conductivity data for the CVD SiC sample, the critical temperature for amorphization at this neutron dose and flux, above which amorphization is not possible, is estimated to be greater than ~125°C.

1. Introduction

Amorphization of silicon carbide has been studied in support of fundamental materials science and in application driven programs such as microelectronics. Several research groups have shown that SiC becomes amorphous during ion-beam irradiation at temperatures between 77 K and room temperature for damage levels equivalent to 0.1–0.5 displacements per atom (dpa) [1–9]. Most of these amorphization studies have used low-energy (<1 MeV) ion-beams [1,2,4–7], with a few researchers using high energy electrons [10–13] to produce the SiC lattice damage.

Recent interest in SiC amorphization has focused on the temperature dependence of the critical dose for amorphization. In situ TEM observation of the critical dose for amorphization as a function of irradiation temperature has been studied using 2 MeV electrons, [11–13] 360 keV argon or 1.5 MeV xenon ions [14–17]. Zinkle and Snead have used 0.56 MeV silicon ions implanted into samples which were then prepared for TEM observation [8,9,18]. In all of these studies, the threshold for amorphization for single crystal SiC was measured as a function of temperature. It was observed that there is a temperature-independent amorphization dose at low temperatures followed by a temperature above which the damage level required to amorphize SiC increases rapidly. In each case an apparent asymptotic increase in the amorphization dose occurred, yielding a 'critical temperature' above which amorphization appears impossible. This critical temperature has been reported to range between 20°C and 70°C for electrons [11,12,19], ~150°C for Si ions [9,18] and ~220°C for Xe ions [15], all with similar damage rates of $\sim 1 \times 10^{-3}$ dpa/s. It is noted that both Weber [14,15] and Matsunaga's [10] work did not observe a significant difference in amorphization threshold between α- and β-SiC, whereas Inui reported a threshold temperature ~50°C higher for faulted β-SiC [12].

While amorphization has been demonstrated for a number of ceramics using electron and ion irradiation, there is very little information on neutron-induced ceramic amorphization. There has been significant work on the microstructural and physical properties of neutron amorphized quartz [20–22], though this crystal to

* Corresponding author. Tel.: +1-423 574 9942; fax: +1-423 576 8424; e-mail: z2n@ornl.gov.

[1] Present address: IBM Thomas J. Watson Research Center, P.O. Box 218, Room 218, Yorktown Heights, NY 10596-0218, USA.

0022-3115/99/$ – see front matter
PII: S0022-3115(99)00023-9

amorphous transition is due to radiolysis rather than due to displaced atoms. Other silicates, such as beryl ($3Beo–Al_2O_3–6SiO_2$), garnet ($Ca_3Al_2Si_3O_{12}$), topaz ($A_{12}(OH)_2SiO_4$) and zircon ($ZrSiO_4$), also amorphize by radiolysis at neutron dose levels equivalent to ~0.6 dpa [23]. It has also been claimed that graphite amorphizes under neutron irradiation [24,25] at dose and temperatures <1 dpa and 200°C, though, as pointed out by Kelly [26], the Raman spectra used as an indication for amorphization is consistent with the formation of in-plane edge dislocation dipoles. Another convincing piece of evidence against neutron induced amorphization of graphite, as quoted by previous authors [24,25] is that the dimensional change continues to behave anisotropically as the dose is increased above the apparent amorphization dose [26]. Diamond, however, has been shown to undergo amorphization during neutron bombardment by several researchers [27–32]. Of interest for diamond and the other amorphized ceramics is the large associated density change. Specifically, the decrease in density upon amorphization is 45% for diamond [27–31], ~15% for quartz [20,33], >6.2% for beryl [23], >5.5 for garnet [23], and >9% for zircon [34]. This swelling can be contrasted with the typical radiation-induced point defect strain in crystalline ceramics of less than a few percent [20].

As stated earlier, there has been no work demonstrating neutron-induced amorphization of SiC. There has been substantial work on the swelling, microstructure and mechanical properties of neutron irradiated SiC, though the majority of this work has been at elevated irradiation temperatures or at fluences apparently too low to induce amorphization. Primak et al. [36] reported irradiating single crystal 6H silicon carbide to 3×10^{24} n/m^2 (fast) at ~30°C in the MTR. The maximum swelling measured using macroscopic means was reported at 1.24%. Pravdyuk et al. [37] measured macroscopic swelling and microscopic lattice expansion of 1.03% following irradiation to 7.2×10^{24} n/m^2 at ~120°C for an unspecified neutron energy spectrum. Other data have been generated at 140°C by Corelli et al. [38] to 7.2×10^{24} n/m^2 ($E > 1$ MeV) which showed approximately 0.5% swelling. It should be noted that Corelli's materials were hot pressed and contained boron and free silicon which affected the rate of swelling as a function of neutron fluence. Above 200°C significant data exists [36,39–45] to high doses in single crystal and stoichiometric polycrystal forms of SiC which exhibit two general trends. First, the swelling of SiC in the 200–1000°C range saturates at a fast neutron fluence of approximately 1×10^{25} n/m^2 ($E > 0.1$ MeV). Second, the amount of swelling appears to linearly decrease with increasing irradiation temperature and approaches zero at 1000°C.

Physical properties such as density, hardness and elastic modulus of amorphized single and polycrystalline SiC have been previously estimated from measurements of surface or buried amorphous layers produced by ion beam irradiation. Specifically, the density has been inferred by surface step height measurements [47–49], by observing the increase in total range with TEM [8,9,17,50], or by X-ray techniques [51,52], yielding a density decrease ranging from about −22% to −15%. The normalized hardness, defined as the ratio of the as-irradiated to unirradiated hardness, (H_i/H_u), [17,48,49,53] and the normalized modulus (E_i/E_u) [17,53] for ion irradiated (amorphous) SiC have likewise ranged in the literature from 45% to 76%, respectively.

2. Experimental

Samples of Cree Systems Inc. 6H alpha single crystal SiC and Morton Advanced Materials CVD SiC were used in this study. The single crystal SiC wafer was purchased with an aluminium doping level of ~5 wppm. All other impurities for the single crystal material were in the wppb range. The CVD SiC is characterized as a highly faulted 3C structure with all impurities, as measured by the manufacturer, in the ppb range with the exception of titanium which is listed as 1.4 wppm. These materials were irradiated in the HT-3 hydraulic rabbit position of the High Flux Isotope Reactor at ORNL in perforated aluminium capsules. The samples were irradiated in contact with ~53°C flowing coolant water at a fast neutron flux of 7.8×10^{18} n/m^2 s ($E > 0.1$ MeV) to a total fluence of 2.6×10^{25} n/m^2 ($E > 0.1$ MeV). This fluence level is equal to a damage level of ~2.6 dpa, assuming a displacement energy (E_d) of 40 eV for both the Si and C sublattices, while it is noted that E_d varies widely in the literature [35]. The single crystal material was irradiated as wafer fragments of 0.34 mm thickness. The CVD SiC was irradiated as a 6-mm diameter, 10-mm long cylinder.

Specimen densities were obtained with density gradient columns using mixtures of tetrabromoethane-methylene iodide or ethylene bromide-bromoform for the unirradiated and irradiated samples, respectively. The accuracy of the measurement was better than 0.001 g/cc and was found to be reproducible in repeated measurements and consistent for duplicate samples. All samples were immersed in hydrofluoric acid for a period greater than 24 h to remove any surface silica prior to measurement. Microindentation hardness and elastic modulus were determined using a Nanoindentor^{TM}-II with a peak loading of 30 mN and a constant loading rate of 1.5 mN/s. The CVD SiC sample was polished with 1 μm diamond paste before indentation. A Buehler Micromet 3 microhardness testing machine was used at 500 g and 1 kg loads to measure the Vickers hardness. The two loads gave essentially the same hardness values. Only the 1 kg load hardness data is reported here. In-

dentation fracture toughness was found using cracks produced with the Vickers indentor. TEM microscopy was performed using a Philips CM-12 microscope on samples which were mechanically thinned and ion-milled with argon ions at 6 keV and an incident angle of 15° using a liquid-nitrogen-cooled stage during milling. After foil perforation, the specimens were milled at 3 keV and 9° for 10 min at ambient temperature to reduce surface amorphization associated with argon implantation. This procedure has been used extensively on ion-implanted SiC and causes minimal surface amorphization.

3. Results and discussion

3.1. Amorphization and disordering of SiC by neutron irradiation

The materials in this study were taken to approximately an order of magnitude higher dose than the 30°C irradiated materials of Ref. [36] mentioned in the introduction. A volumetric change of 10.8% was found for the single crystal material, which is substantially higher than expected due to point defect accumulation. Both single crystal and CVD SiC samples were examined by TEM. Fig. 1 shows an electron diffraction pattern for the single crystal specimen that was irradiated in contact with the HFIR coolant water to a dose of 2.6 dpa. The diffraction pattern shows diffuse rings typical of an amorphous material. There was no indication of diffraction spots anywhere in the sample and no contrast was found during dark field imaging. X-ray analysis (performed on the sample prior to sample thinning for TEM) also showed no evidence of crystallinity [46]. A separate paper analyzes the microstructure of this material and the recrystallization kinetics determined by in situ TEM annealing [46].

A substantial radial temperature gradient occurred during irradiation of the 6 mm diameter CVD SiC cylinder due to the constraint that the nuclear heat generated in the sample was removed through the sample periphery. The periphery of the sample was in contact with the ~53°C coolant water. The effect of this temperature gradient, which will be discussed in some detail in Section 3.3, was to create an amorphous periphery around a crystalline core. Fig. 2 shows an electron diffraction pattern taken approximately 1 mm from the center of the 6 mm cylindrical sample. In this micrograph a combination of diffuse rings and crystalline spots are seen. Dark field imaging in this area yielded spot-reflections on the order of 10 nm in size. Near the center of the sample both bright field images and diffraction patterns were indistinguishable from those of unirradiated material. While this is proof that the sample center remained crystalline, it is not sufficient evidence to rule out the presence of small amorphous islands within a crystalline matrix.

3.2. Physical properties of neutron amorphized SiC

3.2.1. Swelling

Property measurement of the bulk amorphous samples in this study offers several advantages over measurement on the surface or buried layers associated with ion beam amorphized SiC. For example, the density

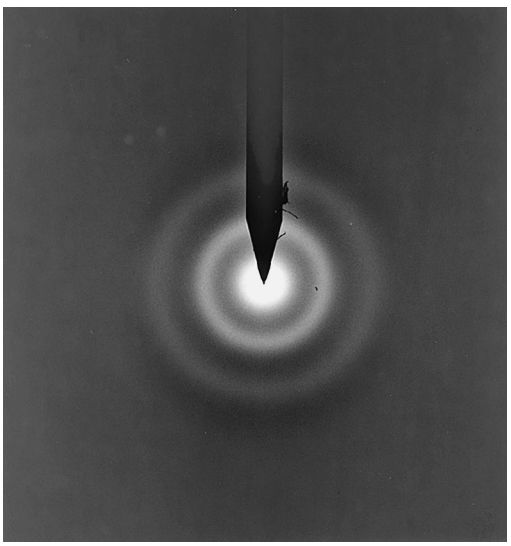

Fig. 1. Electron diffraction pattern of single crystal alpha SiC amorphized by 2.6 dpa neutron irradiation at ~60°C.

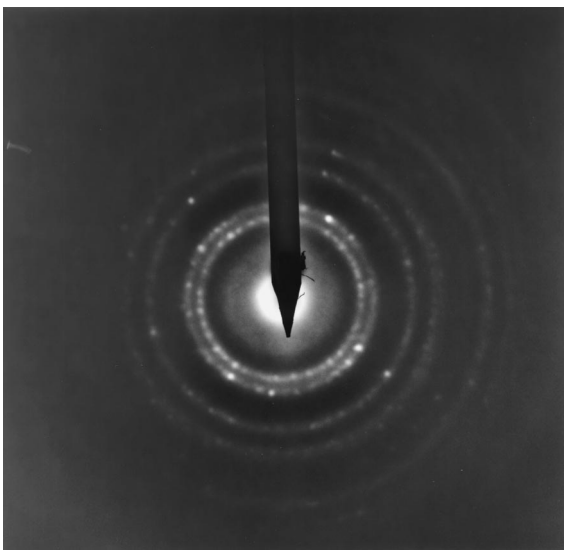

Fig. 2. Electron diffraction pattern of 2.6 dpa neutron irradiated CVD SiC near the crystalline–amorphous transition.

(swelling) can be measured with an uncertainty of ±0.001 g/cc using the density gradient column technique. For the 2.6 dpa irradiated 6H single crystal SiC the density was found to be 2.857 g/cm^3, corresponding to a 10.8% reduction in density from the 3.204 g/cm^3 unirradiated value. It is interesting to note that Snead [9] previously reported a similar decrease in density for hot pressed β-SiC (−10.1% or 2.84 g/cm^3) and sintered α-SiC (−11.8% or 2.79 g/cm^3) which were neutron irradiated to a fluence of $\sim 1.5 \times 10^{26}$ m^{-2} ($E > 0.1$ MeV) at approximately 70°C. However, since the volumetric swelling from ion beam studies was reported to be 15–20%, it was incorrectly assumed that these neutron irradiated samples were only discontinuously amorphous. The difference in amorphous density of hot pressed β-SiC and sintered α-SiC materials and the amorphous density found in this paper for amorphized single crystal α-SiC (2.857 g/cm^3) is thought to be due to the presence of sintering aids (Si and B) in the hot pressed and sintered materials.

The density of the CVD SiC sample was measured to be 2.895 g/cm^3 yielding a density decrease of 9.62% from the unirradiated value (3.203 g/cm^3.) As discussed in the previous section, the periphery of this 6 mm sample was amorphous while the center appeared crystalline by TEM. The measured density is therefore an averaged density of a heterogeneous (crystalline plus amorphous) sample.

3.2.2. Mechanical properties

The bulk nature of these specimens also allows measurement of elastic modulus and hardness without concern for underlying crystalline material influencing the results (i.e. substrate effects). These substrate effects are a common problem for the measurement of hardness and elastic modulus from ion beam modified surface or buried layers. While sensitive volume associated with hardness is defined by the material plastically deformed by the indentor, the elastic modulus as calculated from a microindentation unloading curve [54] is an average modulus integrated over a volume much larger than the plastically deformed volume. For a semi-infinite medium, Samuels and Mulhearn [55] have shown that the elastic–plastic boundary extends hemispherically approximately 10 times the indent depth. For the 30 mN load used in this study, this gives a plastically deformed radius for the amorphous SiC (~170 nm contact depth) of approximately 1.7 microns.

The mechanical properties of both unirradiated and irradiated materials are summarized in Table 1. Using a Nanoindentor-II, as was used in some of the previous ion beam studies [9,17,47], the measured hardness of the neutron amorphized 6H-SiC decreased from 38.7 ± 2 to 21.0 ± 1 GPa, while the elastic modulus decreased from 528 ± 14 to 292 ± 5 GPa. The errors quoted correspond to ±1 standard deviation. The normalized hardness

Table 1
Summary of measured properties for unirradiated and 2.6 dpa SiC irradiated at ~60°C

		Single crystal SiC	CVD SiC
H (GPa); Nano-indentor	Unirradiated	38.7 ± 2	36.2 ± 1.2
	2.6 dpa	21.0 ± 1	23.4 ± 0.6
	H_i/H_{unirr}	54 ± 4%	64.6 ± 3.8%
E (GPa); Nano-indentor	Unirradiated	528 ± 14	500 ± 11
	2.6 dpa	292 ± 45	291 ± 7.5
	H_i/H_{unirr}	55 ± 2%	58.2 ± 1.9%
H (kg/mm^2); Vickers	Unirradiated	2245 ± 107	2330 ± 80
	2.6 dpa	1708 ± 35	1797 ± 75
	H_i/H_{unirr}	76 ± 4%	77 ± 4%
Density (g/cm^3)	Unirradiated	3.204	3.203
	2.6 dpa	2.857	2.895 [a]
	$(\rho_{irr} - \rho_{unirr})/\rho_{unirr}$	10.8%	

[a] Only sample periphery amorphized. Data is not a bulk measurement.

(H_{irr}/H_{unirr}) is measured to be 54 ± 4% which is in approximate agreement with previous estimates [17,48,49,53]. However, the 55 ± 2% normalized modulus is significantly lower than previous estimates obtained on ion-irradiated specimens with the exception of one study which used nanoindentation on a 3 MeV carbon ion irradiated specimen prepared in cross section [56]. This would suggest that substrate effects, which would be minimized for cross-sectional indentation, and eliminated for the bulk amorphous materials of this study, were affecting previously reported elastic modulus measurements.

At a 1 kg load the Vickers hardness for the unirradiated single crystal and CVD SiC was measured to be 2245 ± 107 and 2330 ± 80 kg/mm^2, respectively. The hardness of the Morton CVD SiC at 500 g loading was 2339 ± 100 kg/mm^2 which agrees well with the manufacturer's 500 g quoted hardness of 2500 kg/mm^2. For the single crystal and CVD SiC amorphized samples the (1 kg) Vickers hardness was measured to be 1708 ± 35 and 1797 ± 75 kg/mm^2, respectively. This yields a normalized residual Vickers hardness of 76 ± 3.8% for the single crystal material and 77 ± 4.2% for the CVD SiC. The indentation fracture toughness was calculated for the unirradiated and amorphized single crystal SiC sample using the Evans–Davis model [57] at a Vicker's load of 500 g. The average crack length from a series of 10 indents was used along with the Vicker's hardness data and the elastic modulus measured by microindentation (using the Nanoindentor-II). The indentation fracture toughness, K_c, was calculated to increase from 2.5 MPa/m$^{1/2}$ for the unirradiated material to 3.2 MPa/m$^{1/2}$ for the amorphized SiC.

Figs. 3 and 4 give the hardness and modulus as measured with the Nanoindentor-II along the radius of

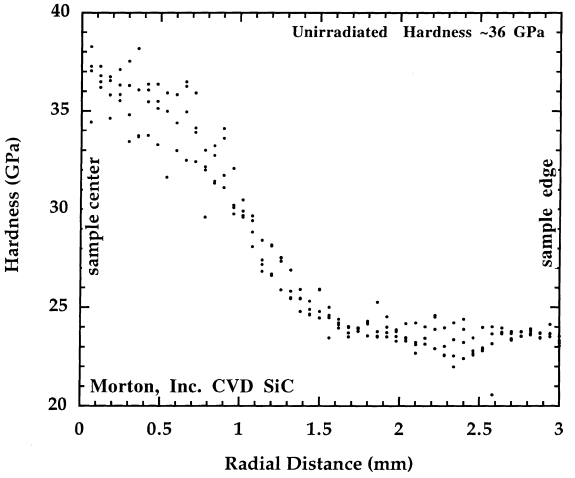

Fig. 3. Hardness as a function of radius for the 2.6 dpa neutron irradiated CVD SiC sample.

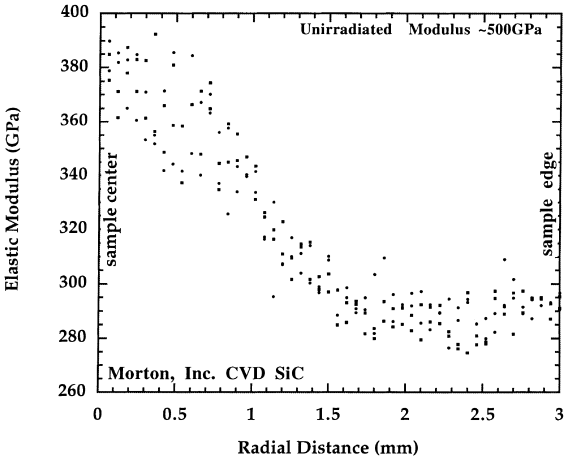

Fig. 4. Elastic modulus as a function of radius for the 2.6 dpa neutron irradiated CVD SiC sample.

the 6 mm diameter CVD SiC sample. From Fig. 3 it is seen that the hardness at the center of the sample (radial distance of zero in figure) is somewhat scattered with mean of 36.2 ± 1.2 GPa which is in agreement with measurements taken on unirradiated material. As the indents move outward radially the hardness falls off rapidly reaching a minimum of 23.4 ± 0.6 GPa, or a normalized hardness of approximately 64.6 ± 3.8%. The elastic modulus shows a similar trend decreasing from 375 ± 10.6 to 291 ± 7.5 GPa. The errors in these cases refer to ±1 standard deviation at radii of 0–0.25 and 2.5–3.0 mm, respectively.

The modulus measured at the center of the sample (Fig. 4) is substantially lower than the 500 GPa modulus measured on an unirradiated sample. Such a decrease in elastic modulus is expected for neutron irradiated ceramics [20]. Specifically, for the same Morton CVD SiC material and measurement technique used in this study, Osborne [58] reported an elastic modulus of ~420 GPa for a 2×20^{25} n/m^2 ($E > 0.1$ MeV) irradiation at ~150°C. It would be expected that for the higher dose material in this study the point defect concentration would be increased and the elastic modulus would be lower. The normalized modulus for the amorphized SiC using the 500 ± 11 GPa unirradiated value is 58.2 ± 1.9%. The scatter associated with the nanoindentation measurement in Figs. 3 and 4 is due in part to the intrinsic machine error and to sample surface roughness. The larger scatter towards the center of the specimen may be attributed to either indent position with respect to crystal grain boundaries or the effect of these grains on the surface finish. As the plastic depth of the indentor was on the order of 200 nm, the small crystallites as discussed in Section 3.1 should not have contributed to the scatter.

3.3. Estimated critical amorphization temperature

As discussed in the introduction, the critical temperature above which amorphization does not occur has been reported to range between 20°C and 220°C [9,11,12,15,18,19] for a damage rate of $\sim 1 \times 10^{-3}$ dpa/s. Below this temperature, the dose required to amorphize SiC appears to approach a constant, although the amorphization dose may be a function of the PKA energy transferred. For example Inui [11,12] reported a threshold dose of 0.5–1.0 dpa for 2 MeV electron irradiation whereas Weber [15] reported a threshold dose of 0.2 dpa for 1.5 MeV Xe^+ ion irradiation. This can be qualitatively explained if one considers that the amorphization in SiC is due to free energy increases associated with point defect accumulation and chemical disordering [59]. Since the amount of chemical disordering per dpa increases with increasing PKA energy, less displacement damage is required to produce amorphization with heavy ions as compared to electrons at all temperatures.

An estimate of the critical temperature for amorphization for fission neutrons can be found using Figs. 3 and 4. From these plots, the point at which the material transforms from crystalline to discontinuously amorphous is at a radius of approximately 1 mm. At 2.6 dpa, for the fast neutron dose rate of $\sim 8 \times 10^{-7}$ dpa/s, this measured transition point defines the threshold amorphization dose for that temperature.

The effect of neutron collisions in ceramics is, among other things, to create lattice vacancies that serve as phonon scattering centers which significantly reduce thermal conductivity [8,9,18,60–62]. From a companion irradiation experiment under identical conditions [63], it is known that a damage level of 0.01 dpa at ~70°C does

not cause amorphization. However, it reduces the room temperature thermal conductivity from 2.56 to 0.31 W/cm K. Irradiation to 0.1 dpa at ~300°C reduces the thermal conductivity to 0.11 W/cm K [63]. Knowing the thermal conductivity as a function of fluence, a simple 1-D thermal transport equation can be used with the measured thermal conductivity data to determine the sample internal temperature as a function of neutron dose. Measured [63] and assumed thermal conductivities are used to generate the curves of Fig. 5. The temperature of the periphery of the sample is taken to be 60°C, to account for the 7°C calculated film temperature drop between the sample edge and the ~53° coolant. At the beginning of irradiation the room temperature thermal conductivity (2.56 W/cm K) is quite high, resulting in a negligible sample internal temperature gradient as seen in the lower curve of Fig. 5. The remaining inset thermal conductivity data are calculated from measured thermal diffusivities [63] of materials irradiated at the same conditions as the amorphized material of this study. However, at 0.1 dpa the conductivity is assumed to be 0.1 W/cm K through comparison with a 0.1 dpa irradiation at 300°C which yielded 0.11 W/cm K. Also note that room temperature thermal conductivity values are used in Fig. 5. Using these room temperature thermal conductivity values, which are slightly greater than the thermal conductivities at temperature, will yield slightly lower internal temperatures (~4%). Accurate data on thermal conductivity as a function of both dose and temperature for SiC is not yet available.

As the thermal conductivity of the 6 mm SiC sample of this study degrades with irradiation the internal temperature increases. At some damage level the periphery of the sample becomes amorphous and the thermal conductivity further decreases to ~0.042 W/cm K [63]. This measurement was on the incompletely amorphized CVD SiC sample and most likely gave a somewhat higher thermal conductivity than if the sample had been fully amorphous. A future measurement of a fully amorphous sample is therefore desirable. Assuming concentric cylinders with distinct thermal conductivity for the crystalline and amorphous regions, the upper curve of Fig. 5 defines the temperature profile for the sample at 2.6 dpa. Assuming transition point from crystalline to discontinuously amorphous material at 1 mm, yields an estimate for the temperature threshold for this 2.6 dpa and $\sim 8 \times 10^{-7}$ dpa/s irradiation. This ~125°C estimate is considered a lower limit for the threshold amorphization temperature.

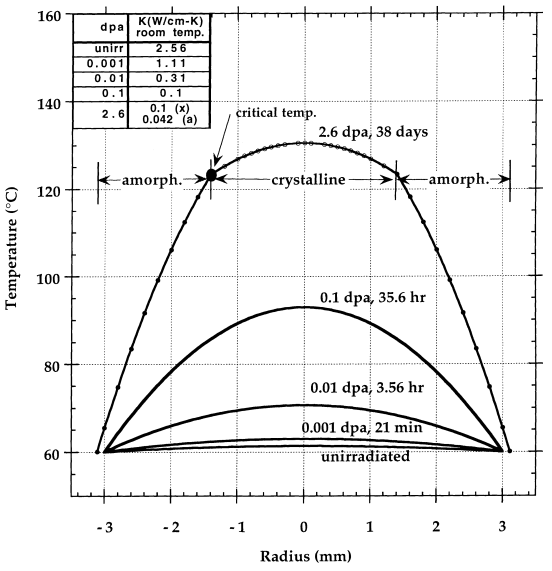

Fig. 5. Internal temperature as a function of dose for the neutron irradiated CVD SiC sample.

This value for the critical amorphization temperature is in reasonable agreement with the ~150°C critical amorphization temperature found by Zinkle [9,18] and Snead [9,18] who used energetic silicon ions at 1×10^{-3} dpa/s and is intermediate between the 20–70°C critical temperature found using 2 MeV electrons [11,12,19] and ~220°C for 1.5 MeV Xe ions [15] also using a displacement rate of 1×10^{-3} dpa/s. The similarity with the silicon ion and the dissimilarity with the electron and xenon ion irradiations can be qualitatively explained considering the nature of the cascades for the various ions. The silicon ion PKA energy is roughly similar with that imparted by an energetic neutron while the average PKA energies for the xenon ion irradiations is substantially greater. Conversely, the electron can only impart enough energy in an elastic collision with the Si or C atoms to create simple Frenkel pairs. However, other explanations exist for the difference in measured amorphization temperature thresholds. As discussed elsewhere [8], the Xenon and electron irradiation used the 'in situ' method where the amorphizing sample was imaged on a thin TEM foil during irradiation. The silicon ion implantations were 'ex situ' measurements where TEM samples were prepared following irradiation. For both of these techniques the potential exists for stress fields altering the results, while the in situ measurement has the added potential complication of the surface acting as a sink for migrating defects.

4. Conclusions

A clear demonstration of the amorphization of silicon carbide caused by the elastic collisions of fast neutrons has been made. Due to the bulk nature of the amorphized material accurate data can be obtained on certain mechanical properties and compared with data from previous ion-beam irradiations. While the hardness data generated in this study falls within the somewhat

wide range in hardness values previously reported, both the previously reported density and elastic modulus of amorphized SiC appear to be substantially different from the actual values. High purity single crystal alpha SiC and high purity polycrystalline beta SiC irradiated to 2.6 dpa at ~60°C have transformed from the crystalline state with a density of 3.203 ± 0.001 to an amorphous state with 10.8% lower density. Using a nanoindentation technique the normalized hardnesses for the single crystal and polycrystalline material are about 54% and 65% of the unirradiated values, respectively, while the normalized elastic modulii are about 55% and 58%, respectively. Vickers normalized hardness was ~76% for amorphous single and polycrystal material. An increase in the indentation fracture toughness from 2.5 to 3.2 $MPa/m^{1/2}$ is also observed upon SiC amorphization. Using measured values of thermal conductivity for irradiated crystalline SiC and the amorphized SiC the lower limit for the threshold temperature for amorphization of SiC by fission neutrons at 2.6 dpa and $\sim 8 \times 10^{-7}$ dpa/s was estimated to be ~125°C. This estimate is in reasonable agreement with previous silicon ion irradiations.

Acknowledgements

This work was conducted for the Department of Energy Office of Fusion Energy by members of the Lockheed Martin Energy Research Corporation under contract DE-AC05-960OR22464.

References

[1] R.R. Hart, H.L. Dunlap, O.J. Marsh, Radiat. Eff. 9 (1971) 261.
[2] J.A. Edmond, R.F. Davis, S.P. Withrow, K.L. More, J. Mater. Res. 3 (1988) 321.
[3] C.W. White et al., Mater. Sci. Rep. 4 (1989) 41.
[4] J.M. Williams, C.J. McHargue, B.R. Appleton, Nucl. Instrum. Meth. 209&210 (1983) 317.
[5] J.A. Spitznagel et al., Nucl. Instrum. Meth. B 16 (1986) 237.
[6] N.G. Chechenin et al., Nucl. Instrum. Meth. B 65 (1992) 341.
[7] L.L. Horton et al., Nucl. Instrum. Meth. B 65 (1992) 345.
[8] L.L. Snead, S.J. Zinkle, in: I.M. Robertson et al. (Eds.), MRS Symposium on Microstructure of Irradiated Materials, Boston, MA, vol. 373, Materials Research Society, Pittsburgh, PA, 1995, p. 377.
[9] L.L. Snead, S.J. Zinkle, in: I.M. Robertson et al. (Eds.), Microstructure Evolution During Irradiation, MRS Symposium Proceedings, vol. 439, Materials Research Society, Pittsburgh, PA, 1997, p. 595.
[10] A. Matsunaga, C. Kinoshita, K. Nakai, Y. Tomokiyo, J. Nucl. Mater. 179–181 (1991) 457.
[11] H. Inui, H. Mori, T. Sakata, Philos. Mag. B 66 (1992) 737.
[12] H. Inui, H. Mori, H. Fujita, Philos. Mag. B 61 (1990) 107.
[13] C. Kinoshita et al., Proceedings of the 11th International Conference on Electron Microscopy, Japanese Society of Electron Microscopy, 1986.
[14] W.J. Weber, L.M. Wang, Nucl. Instrum. Meth. B 106 (1995) 298.
[15] W.J. Weber, L.M. Wang, N. Yu, Nucl. Instrum. Meth. B 116 (1996) 322.
[16] W.J. Weber, N. Yu, Proceedings of the International Conference on Defects in Insulating Materials, 1996.
[17] W.J. Weber, N. Yu, L.M. Wang, N.J. Hess, J. Nucl. Mater. 244 (1997) 258.
[18] S.J. Zinkle, L.L. Snead, Nucl. Instrum. Meth. B 116 (1996) 92.
[19] H. Inui, H. Mori, H. Fujita, Acta Metall. 37 (1989) 1337.
[20] R.A. Wullaert, in: J.F. Kircher, R.E. Bowman (Eds.), Effects of Radiation on Materials and Components, Reinhold, London, 1964, p. 277.
[21] E. Lell, N.J. Kreidl, J.R. Hensler, in: J.E. Burke (Ed.), Progress in Ceramic Science, vol. 4, Pergamon, New York, 1966, p. 1.
[22] F.W. Clinard Jr., L.W. Hobbs, in: R.A. Johnson, A.N. Orlov (Eds.), Physics of Radiation Effects in Crystals, Elsevier, Amsterdam, 1986, p. 387.
[23] M.C. Wittels, F.A. Sherrill, ORNL Solid State Division annual progress report for period ending 31 August 1959, Report ORNL-2829, 1959.
[24] T. Tanabe, S. Muto, G. Y, K. Niwase, J. Nucl. Mater. 175 (1989) 258.
[25] K. Niwase, K. Nakamura, T. Shikama, T. Tanabe, J. Nucl. Mater. 170 (1990) 106.
[26] B.T. Kelly, J. Nucl. Mater. 172 (1990) 237.
[27] E.R. Vance, H.J. Milledge, A.T. Collins, J. Phys. D 5 (1972) L40.
[28] V.Y. Karasov et al., Sov. Phys. Solid State 26 (1984) 1739.
[29] E.R. Vance, J. Phys. C 4 (1971) 257.
[30] D.T. Keating, Acta Crystallogr. 16 (1963) A113.
[31] D.T. Keating, J. Phys. Chem. Solids 29 (1968) 771.
[32] V.A. Nikolaenko, V.G. Gordeev, Radiat. Eff. Def. Solids 139 (1996) 183.
[33] J.R. Gilbreath, O.C. Simpson, Argonne National Laboratory Report, ANL-4888, 1953.
[34] J.H. Crawford, M.C. Wittels, Second International Conference on Peaceful Uses of Atomic Energy, Geneva, Switzerland, 1958, p. 300.
[35] S.J. Zinkle, C. Kinoshita, in: Proc. Int. Workshop on Defect Production, Accumulation and Materials Performance in Irradiation Environment, Davos, Switzerland, 1997, J. Nucl. Mater. 251 (1997) 201.
[36] W. Primak, L.H. Fuchs, P.P. Day, Phys. Rev. 103 (1956) 1184.
[37] N.F. Pravdyuk, V.A. Nikolaenko, V.I. Kapuchin, V.N. Kusnetsov, in: D.J. Littler (Ed.), Properties of Reactor Materials and the Effects of Radiation Damage Proceedings, Butterworths, London, 1962, p. 57.
[38] J.C. Corelli, J. Hoole, J. Lazzaro, C.W. Lee, J. Am. Ceram. Soc. 66 (1983) 529.
[39] R. Blackstone, E.H. Voice, J. Nucl. Mater. 39 (1971) 319.
[40] G.W. Hollenberg et al., J. Nucl. Mater. 219 (1995) 70.
[41] R.J. Price, J. Nucl. Mater. 46 (1973) 268.

[42] R.J. Price, J. Nucl. Mater. 48 (1973) 47.
[43] R.J. Price, J. Nucl. Mater. 33 (1969) 17.
[44] R.P. Thorne, V.C. Howard, Proc. Br. Ceram. Soc. 7 (1967) 439.
[45] R. Mathews, J. Nucl. Mater. 51 (1974) 203.
[46] L.L. Snead, S.J. Zinkle, J.C. Hay, M.C. Osborne, Nucl. Instrum. Meth. B 141 (1997) 123.
[47] C.J. McHargue, J.M. Williams, Nucl. Instrum. Meth. B 80&81 (1993) 889.
[48] C.J. McHargue et al., Mater. Sci. Eng. 69 (1985) 123.
[49] C.J. McHargue, C.S. Yust, J. Am. Ceram. Soc. 67 (1984) 117.
[50] J. Bentley, L.J. Romana, L.L. Horton, C.J. McHargue, in: G.S. Was, L.E. Rehn, D.M. Follstaedt (Eds.), Phase Formation and Modification by Beam-Solid Interactions. Materials Research Society, 1992, p. 363.
[51] W. Bolse, J. Conrad, T. Rodle, T. Weber, Surf. Coat. Techn. 74&75 (1995) 927.
[52] V. Heera, J. Stoemenos, R. Kogler, W. Skorupa, J. Appl. Phys. 77 (1995) 999.
[53] C.J. McHargue, D.L. Joslin, J.M. Williams, Nucl. Instrum. Meth. B 46 (1990) 185.
[54] W.C. Oliver, G.M. Pharr, J. Mater. Res. 7 (1992) 1564.
[55] L.E. Samuels, T.O. Mulhearn, J. Mech. Phys. Solids 5 (1957) 125.
[56] L.L. Snead, S.J. Zinkle, D. Steiner, J. Nucl. Mater. 191–194 (1992) 560.
[57] A.G. Evans, in: S.W. Frieman (Ed.), Proceedings of the Eleventh National Symposium on Fracture Mechanics Part II, ASTM, Philadelphia, 1979, p. 112.
[58] M.C. Osborne, L.L. Snead, J.C. Hay, J. Mater. Res., submitted.
[59] A.T. Motta, D.R. Olander, Acta Metall. Mater. 38 (1990) 2175.
[60] P.G. Klemens, in: F. Seitz, D. Turnbull (Eds.), Solid State Physics, vol. 7, Academic Press, New York, 1958, p. 1.
[61] P.G. Klemens, In: R.P. Tye (Ed.), Thermal Conductivity, vol. 1, Academic Press, New York, 1969, p. 1.
[62] P.G. Klemens, G.F. Hurley, F.W. Clinard Jr., in: G.L. Kulcinski, N.M. Burleigh (Eds.), Proceedings of 2nd Topical Meeting on the Technology of Controlled Nuclear Fusion, CONF-760935. National Tech. Inform. Service, Springfield, VA, 1976, p. 957.
[63] L.L. Snead, S.J. Zinkle, D.P. White, J. Nucl. Mater. submitted.